ISSN 1674-1056
http://cpb.iphy.ac.cn
http://iopscience.iop.org/cpb
中国物理 B
Chinese Physics
中国物理 Chinese Physics B

Inverse spin Hall effect in ITO/YIG exited by spin pumping and spin Seebeck experiments

Kejian Zhu(朱科建), Weijian Lin(林伟坚), Yangtao Su(苏仰涛), Haibin Shi(石海滨), Yang Meng(孟洋), Hongwu Zhao(赵宏武)

Citation: Chin. Phys. B . 2019, 28(1): 017201. **doi:** 10.1088/1674-1056/28/1/017201
Journal homepage: http://cpb.iphy.ac.cn; http://iopscience.iop.org/cpb

What follows is a list of articles you may be interested in

Spin Seebeck effect and spin Hall magnetoresistance in the Pt/$Y_3Fe_5O_{12}$ heterostructure under laser-heating

Shuanhu Wang(王拴虎), Gang Li(李刚), Jianyuan Wang(王建元), Yingyi Tian(田颖异), Hongrui Zhang(张洪瑞), Lvkuan Zou(邹吕宽), Jirong Sun(孙继荣), Kexin Jin(金克新)

Chin. Phys. B . 2018, 27(11): 117201. **doi:** 10.1088/1674-1056/27/11/117201

Electrical controllable spin valves in a zigzag silicene nanoribbon ferromagnetic junction

Lin Zhang(张林)

Chin. Phys. B . 2018, 27(6): 067203. **doi:** 10.1088/1674-1056/27/6/067203

Spin flip in single quantum ring with Rashba spin-orbit interation

Duan-Yang Liu(刘端阳), Jian-Bai Xia(夏建白)

Chin. Phys. B . 2018, 27(3): 037201. **doi:** 10.1088/1674-1056/27/3/037201

Spin transport in a chain of polygonal quantum rings with Dresselhaus spin-orbit coupling

Han-Zhao Tang(唐翰昭), Xiao-Teng Yao(要晓腾), Jian-Jun Liu(刘建军)

Chin. Phys. B . 2017, 26(11): 117203. **doi:** 10.1088/1674-1056/26/11/117203

The origin of spin current in YIG/nonmagnetic metal multilayers at ferromagnetic resonance

Yun Kang(康韵), Hai Zhong(钟海), Runrun Hao(郝润润), Shujun Hu(胡树军), Shishou Kang(康仕寿), Guolei Liu(刘国磊), Yin Zhang(张引), Xiangrong Wang(王向荣), Shishen Yan(颜世申), Yong Wu(吴勇), Shuyun Yu(于淑云), Guangbing Han(韩广兵), Yong Jiang(姜勇), Liangmo Mei(梅良模)

Chin. Phys. B . 2017, 26(4): 047202. **doi:** 10.1088/1674-1056/26/4/047202

Inverse spin Hall effect in ITO/YIG exited by spin pumping and spin Seebeck experiments*

Kejian Zhu(朱科建)[1,2], Weijian Lin(林伟坚)[1,2], Yangtao Su(苏仰涛)[1,2], Haibin Shi(石海滨)[1,2], Yang Meng(孟洋)[1,2], and Hongwu Zhao(赵宏武)[1,2,3,†]

[1] *Beijing National Laboratory for Condensed Matter Physics, Institute of Physics, Chinese Academy of Sciences, Beijing* 100190, *China*
[2] *School of Physical Sciences, University of Chinese Academy of Sciences, Beijing* 100049, *China*
[3] *Songshan Lake Materials Laboratory, Dongguan* 523808, *China*

(Received 28 September 2018; revised manuscript received 31 October 2018; published online 12 December 2018)

Spin currents, which are excited in indium tin oxide (ITO)/yttrium iron garnet (YIG) by the methods of spin pumping and spin Seebeck effect, are investigated through the inverse spin Hall effect (ISHE). It is demonstrated that the ISHE voltage can be generated in ITO by spin pumping under both in-plane and out-of-plane magnetization configurations. Moreover, it is observed that the enhancement of spin Hall angle and interfacial spin mixing conductance can be achieved by an appropriate annealing process. However, the ISHE voltage is hardly seen in the presence of a longitudinal temperature gradient. The absence of the longitudinal spin Seebeck effect can be ascribed to the almost equal thermal conductivity of ITO and YIG and specific interface structure, or to the large negative temperature dependent spin mixing conductance.

Keywords: spin pumping, spin Seebeck effect, inverse spin Hall effect

PACS: 72.25.Dc, 72.25.Mk, 46.40.Ff **DOI:** 10.1088/1674-1056/28/1/017201

1. Introduction

The generation and detection of spin currents play a critical role in the field of spintronics. To date, the spin pumping effect and the spin Seebeck effect (SSE) are two widely used approaches to generate spin currents in nonmagnetic /ferromagnetic heterostructures.[1–10] The spin current can be detected by the inverse spin Hall effect (ISHE) which converts a spin current into an electric voltage through spin–orbit coupling (SOC) in nonmagnetic materials.[11–21] Usually, some 5d metals are used as spin detector materials due to their enhanced intrinsic SOC and large spin Hall angle θ_{SH} (typical 0.01–0.1), such as Pt and Au.[1,2,7–11] Meanwhile, some oxides with larger resistivity are proposed to serve as spin detectors in order to achieve larger ISHE signal, according to the $V_{ISHE} \propto \rho_c \theta_{SH} I_s$ relationship.[22–25] Fujiwara *et al.* reported that IrO_2 can be used for spin detection and the spin Hall resistivity $\rho_{SH} = \rho_c \theta_{SH}$ of IrO_2 is even larger than that of typical heavy metals and their alloys.[22] Qiu *et al.* observed a strong ISHE signal in indium tin oxide (ITO)/yttrium iron garnet (YIG) bilayers by spin pumping, and found that the mixing conductance at the ITO/Py interface is very close to that of a metal/metal interface.[23,24] Further, a smaller V_{ISHE} in IrO_2/YIG was achieved in the longitudinal SSE (LSSE) configuration, and attributed to the weak interfacial spin mixing conductance.[25] So far, there are only a limited number of reports on using oxides for spin detection, and more experimental investigations are essential to realize high conversion of spin current into electric voltage by different approaches.

ITO is the most widely used transparent oxide that shows a much higher resistivity than metals, which is beneficial to attain a large spin Hall resistivity. In this study, we investigate the generation of spin current in ITO/YIG bilayer by the method of spin pumping and LSSE. The ISHE of ITO/YIG driven by spin pumping under different magnetization configurations was observed, demonstrating that ITO can be used as a spin detect material. However, we did not observe the ISHE signal in the presence of a longitudinal temperature gradient in ITO/YIG, which is probably due to almost the same thermal conductivities of ITO and YIG and particular interface structure.

2. Experimental details

First, a 100-nm-thick ITO film was deposited on single crystalline (111) YIG films by magnetron sputtering at room temperature. The YIG film of 3.23 μm thickness was grown by the method of liquid phase epitaxy on $Gd_3Ga_5O_{12}$ (GGG) substrates. Then, the stripe (length: 3 mm, width: 0.3 mm) and Hall bar (length: 5 mm, width: 3 mm, arm width: 0.3 mm) structures of the ITO layer were prepared by standard photolithography for spin pumping and SSE measurements, respectively, as shown in Fig. 1(a). In addition, a Pt layer of 10 nm thickness with the same stripe and Hall bar structures

*Project supported by the National Key Basic Research Project of China (Grant No. 2016YFA0300600), Chinese Academy of Sciences (Grant No. KJCX2-YW-W24), the Young Scientists Fund of the National Natural Science Foundation of China (Grant No. 11604375), and the Laboratory of Microfabrication of Institute of Physics, Chinese Academy of Sciences.

†Corresponding author. E-mail: hwzhao@aphy.iphy.ac.cn

© 2019 Chinese Physical Society and IOP Publishing Ltd

was prepared on YIG as a reference sample. Silver colloid was employed to electrically connect the ITO surface and Pt wire as an electrode, and then was baked at 423 K for about 30 min to achieve Ohmic contacts. For the spin pumping experiment, a microwave excitation with the frequency of 3.5 GHz was generated and applied to the ITO/YIG samples by a microwave line with diameter around 30 μm. A magnetic field $\boldsymbol{H}$ was provided by a two-dimensional (2D) vector field. The ferromagnetic resonance (FMR) spectra of all the samples were taken by a N5230A PNA-L network analyzer from Agilent Technologies. The DC voltage induced by ISHE in ITO was measured as a function of H. For the LSSE experiment, a longitudinal temperature gradient ∇T_z was formed out of the plane in the z direction by sandwiching the sample between a large Cu block and a heater.[26] The temperature difference ΔT_z is defined as the corresponding temperature difference between the ITO surface and the bottom of the sample substrate. Before measurements, the transport setup was mounted in a cryostat of low vacuum to effectively reduce the interference signals outside. All of the experiments were performed at room temperature.

3. Results and discussion

Initially, a 20 mW microwave excitation of 3.5 GHz was applied on an as-prepared ITO(100 nm)/YIG sample (Fig. 1(a)). The ISHE voltage $V_{\rm ISHE}$ was measured as a function of magnetic field H with $\boldsymbol{H}$ along the y axis in the film plane. In Fig. 1(b), it is noted that two anti-symmetric voltage peaks with opposite signs appear around ±700 Oe. The ISHE voltage exited by spin pumping is ascribed to the generation of spin currents in ITO, which is generated by spin pumping in YIG and injected into the adjacent ITO layer due to ISHE.[7–9] The single peak feature is different from the multiple peak characteristics reported in ITO/La:YIG, which was attributed to the spin wave resonant effect.[23] For comparison, the magnetic field dependence of $V_{\rm ISHE}$ of a Pt(10 nm)/YIG sample is shown in Fig. 1(b). Note that the sign of the voltage peak of Pt/YIG is reversed relative to that of ITO/YIG, which is attributed to the opposite sign of $\theta_{\rm SH}$.

Figure 1(c) shows the FMR linewidths of the YIG, Pt/YIG, and as-prepared ITO/YIG structure as a function of the microwave frequency. It is shown that the linewidth increases linearly with the frequency, from which the damping parameter α can be estimated to be 1.44×10^{-2} and 1.45×10^{-2} for the as-prepared ITO/YIG and Pt/YIG structure, respectively.[27,28] In general, the spin Hall angle $\theta_{\rm SH}$ and interfacial spin mixing conductance $g_{\uparrow\downarrow}$ can be deduced from

$$V_{\rm ISHE} = \frac{-e\theta_{\rm SH}}{\sigma_{\rm NM}t_{\rm NM}}\lambda_{\rm SD}\tanh\left(\frac{t_{\rm NM}}{2\lambda_{\rm SD}}\right)g_{\uparrow\downarrow}fLP\left(\frac{\gamma h_{\rm rf}}{4\pi\alpha f}\right)^2, \quad (1)$$

$$g_{\uparrow\downarrow} = \frac{4\pi M_{\rm s}t_{\rm YIG}}{g\mu_{\rm B}}\left(\alpha_{\rm NM/YIG}-\alpha_{\rm YIG}\right), \quad (2)$$

where $\lambda_{\rm SD}$ is the material's specific spin diffusion length, $\sigma_{\rm NM}$, $t_{\rm NM}$, and L are the conductivity, thickness, and length of the nonmagnetic layer, respectively. $M_{\rm s}$ and $t_{\rm YIG}$ are the saturation magnetization and the effective thickness of the YIG films, and g and $\mu_{\rm B}$ are the Lande factor and Bohr magneton, respectively.[9,11,29,30]

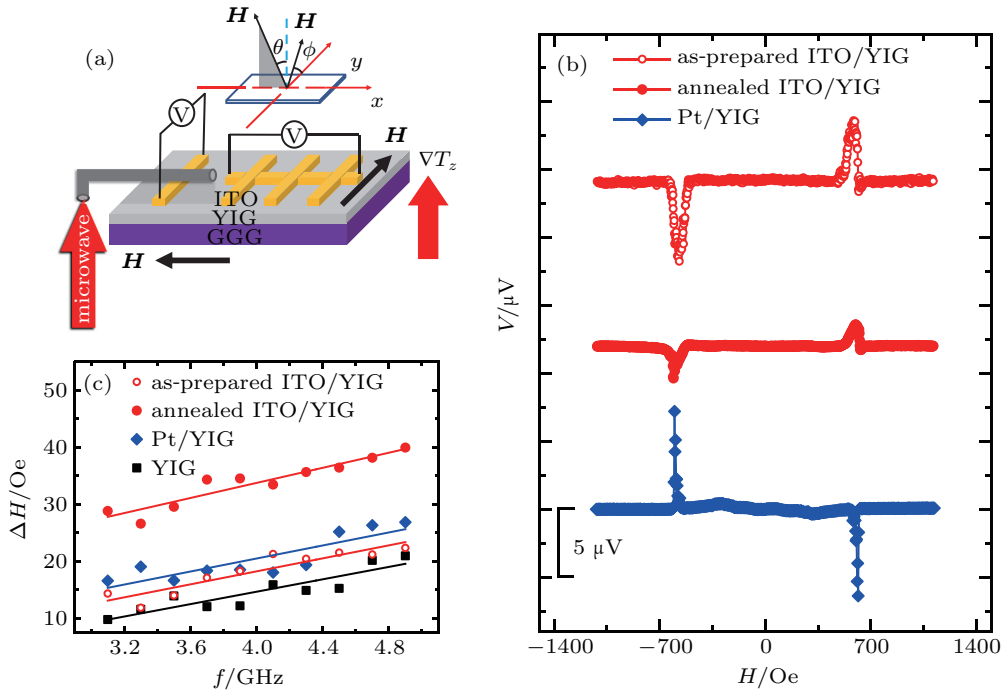


Fig. 1. (a) Schematic diagram of the ITO(100 nm)/YIG sample and electrical measurement geometry. The stripe and the Hall bar were used for spin pumping and LSSE measurements, respectively. (b) ISHE voltage as a function of H along y axis for the as-prepared ITO/YIG, annealed ITO/YIG, and Pt/YIG. (c) FMR linewidths of YIG, Pt/YIG, as-prepared ITO/YIG, and annealed ITO/YIG structure as a function of the microwave frequency.

Consequently, θ_{SH} and $g_{\uparrow\downarrow}$ of Pt/YIG are calculated to be 8.46×10^{-2} and 8.06×10^{18} m^{-2}, which are comparable to the values in the previous reports,[11,31] indicating the validity and reliability of the spin pumping measurement. For the as-prepared ITO/YIG, θ_{SH} and $g_{\uparrow\downarrow}$ are calculated to be -2.88×10^{-4} and 7.66×10^{18} m^{-2}, respectively. In the previous reports, θ_{SH} and $g_{\uparrow\downarrow}$ of ITO/Py and IrO_2/YIG were estimated to be 0.0065 ± 0.001 and $(1.1 \pm 0.2) \times 10^{19}$ m^{-2}, 4×10^{-2} and 1.2×10^{16} m^{-2}, respectively.[22,24,25] By comparison, the absolute value of θ_{SH} of ITO/YIG is much smaller than that of Pt/YIG (8.46×10^{-2}) and IrO_2/YIG (4×10^{-2}). Meanwhile, $g_{\uparrow\downarrow}$ of ITO/YIG is comparable to that of Pt/YIG, and even two orders of magnitude larger than that of IrO_2/YIG. The typical value of resistivity of the as-prepared ITO in our experiment is about 4.46×10^{-4} Ω·m. Therefore, the large ISHE signal of the as-prepared ITO/YIG arises from the large value of $g_{\uparrow\downarrow}$ of ITO/YIG and the large resistivity of ITO, according to Eq. (1). Furthermore, this conclusion prompts that the ISHE signal may be enhanced by annealing the ITO/YIG sample so as to further vary $g_{\uparrow\downarrow}$ and resistivity of ITO. To validate this assumption, we annealed the ITO/YIG sample at 340 °C in oxygen atmosphere for 10 min, then measured the transport properties. In Fig. 1(b), it is seen that the ISHE voltage of the annealed ITO/YIG structure is reduced compared with that of the as-prepared ITO/YIG. The θ_{SH} and $g_{\uparrow\downarrow}$ of the annealed ITO/YIG sample are estimated to be -2.92×10^{-3} and 3.47×10^{19} m^{-2}, respectively, which are obviously larger than those of the as-prepared sample (-2.88×10^{-4} and 7.66×10^{18} m^{-2}). After the annealing process, the ITO film resistivity decreases from 4.46×10^{-4} Ω·m for the as-prepared ITO to about 8.62×10^{-6} Ω·m. The different trends of variation of θ_{SH}, $g_{\uparrow\downarrow}$, and resistivity of ITO jointly lead to the reduced ISHE signal of the annealed ITO/YIG. Therefore, it is expected to achieve higher spin-to-charge conversion by optimizing the annealing temperature in the future.

To obtain insight of the characteristics of ISHE, we measured the angular dependence of V_{ISHE} of the as-prepared ITO/YIG. Figure 2(a) shows the results of V_{ISHE} as a function of H at different ϕ with $\boldsymbol{H}$ applied in the YIG film plane. As ϕ changes from 270° to 180°, V_{ISHE} at the resonant field (around 700 Oe) is gradually reduced from the maximum to zero, and reverses its sign as ϕ changes from 180° to 90°. The values of H_{res} and V_{ISHE} in Fig. 2(a) have been extracted to be plotted as a function of ϕ, as shown in Figs. 2(b) and 2(c), respectively. It is obviously seen that H_{res} exhibits a $\cos 2\phi$ dependence, as a result of a weak uniaxial in-plane magnetic anisotropy field of YIG (about 72.53 Oe).[32] For V_{ISHE}, the obvious $\sin\phi$ relation is a characteristic of ISHE since $V \propto J_s \times M$.[8,23] Figure 2(d) shows the microwave power dependence of V_{ISHE} at $\phi = 270°$. It can be seen that V_{ISHE} increases linearly with P, which was expected for the ISHE induced by spin pumping.[8,33] Thus, these results confirm that the observed ISHE voltage arises from FMR spin pumping due to the magnetic field applied in the YIG film plane. For the annealed ITO/YIG samples, the similar results were qualitatively obtained.

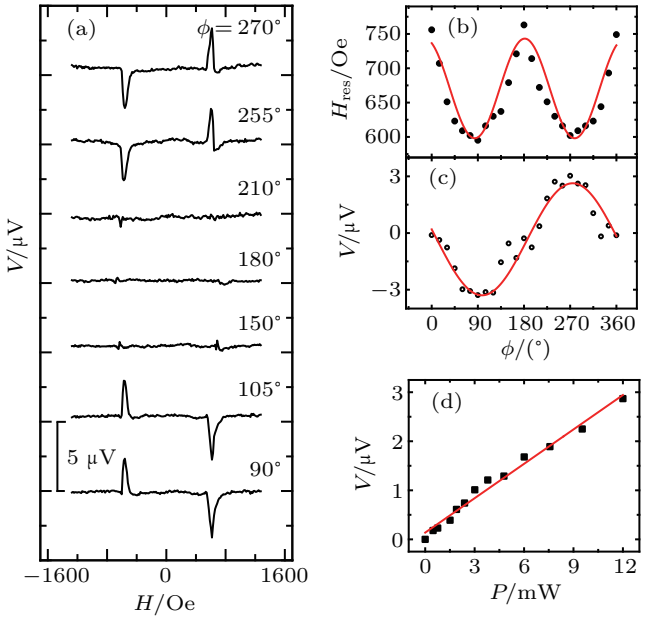


Fig. 2. (a) Angular dependent V_{ISHE}–H characteristics of ITO/YIG with in-plane magnetic field. (b) H_{res} and (c) V_{ISHE} as a function of ϕ. (d) V_{ISHE} as a function of microwave excitation power P.

To further investigate the dependence of the spin polarization vector on ISHE, the V_{ISHE} signal of the as-prepared ITO/YIG was measured with the magnetic field applied out-of-plane. Figure 3(a) shows the field dependence of V_{ISHE} at various θ. It is clearly seen that V_{ISHE} increases from the minimum to maximum as θ changes from 0° to 90°, and H_{res} varies in the opposite trend. The values of H_{res} and V_{ISHE} in Fig. 3(a) are plotted as a function of θ in Figs. 3(b) and 3(c), respectively. The similar angular symmetries for H_{res} and V_{ISHE} exhibit the out-of-plane ISHE behaviors. By comparison of Figs. 2(b) and 3(b), it is noted that the H_{res} for the out-of-plane geometry is much larger than that of in-plane due to the extra force to counteract the demagnetization field of YIG. Due to the enhanced demagnetizing field with $\boldsymbol{H}$ applied out-of-plane, the direction of the magnetization of YIG does not always follow that of $\boldsymbol{H}$,[8] leading to the deviation of the V_{ISHE}–θ curve from $\sin\theta$ as shown in Fig. 3(b). As a result, the angular dependences of H_{res} and V_{ISHE} measured in both in-plane and out-of-plane geometries indicate that the spin current can be generated in YIG by the spin pumping excitation, and ITO can be used as a spin detecting material.

Beside the spin pumping effect, it is well known that spin currents can also be generated by a temperature gradient in NM/FM heterostructures, which is manifested as the LSSE.[34–36] To explore the efficient method of generating

spin currents, we studied the ISHE by applying a longitudinal temperature gradient to the as-prepared ITO/YIG structure.[28] Figure 4 shows the thermal voltage as a function of the magnetic field. It is obvious that the ISHE signal is absent in the presence of the longitudinal temperature differences of 50 K and 100 K, revealing that the spin current is hardly excited through heat gradient in the as-prepared ITO/YIG. This is also true for the annealed ITO/YIG. In contrast, a giant ISHE signal can be achieved in the Pt/YIG structure when a temperature difference ΔT_z of 50 K is applied, as illustrated in Fig. 4.[2,37]

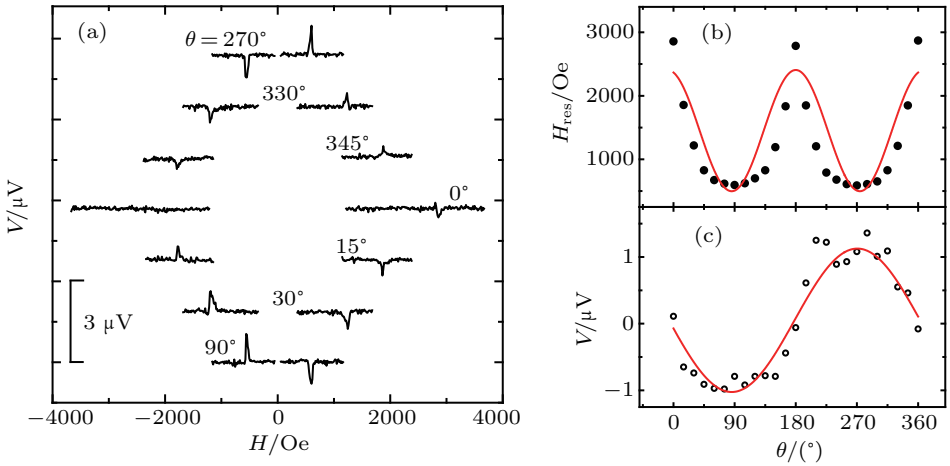


Fig. 3. (a) Angular dependent $V_{\rm ISHE}$–H characteristics of ITO/YIG with out-of-plane magnetic field. (b) $H_{\rm res}$ and (c) $V_{\rm ISHE}$ as a function of θ.

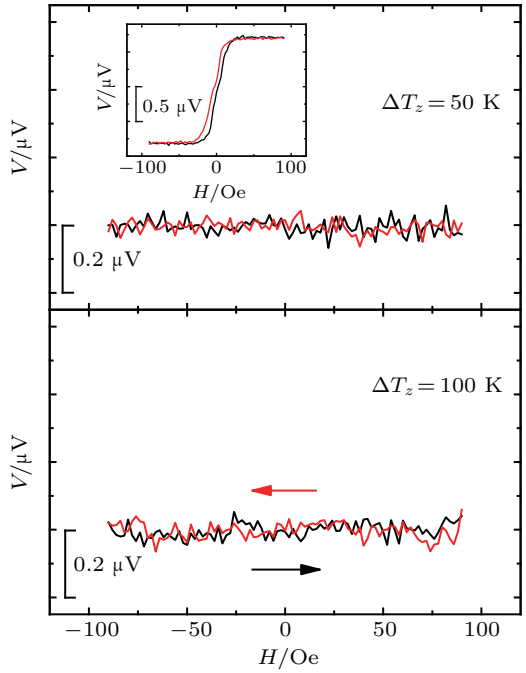


Fig. 4. The H dependence of thermal voltage of ITO/YIG at (a) $\Delta T_z = 50$ K and (b) 100 K. Insert in (a) shows the V–H curves of Pt/YIG at $\Delta T_z = 50$ K.

We suggest that almost the same thermal conductivity of the ITO and substrate (ITO: $\sim$ 5.95 W·m^{-1}·K^{-1}, YIG: 7.4 W·m^{-1}·K^{-1}, GGG: 9 W·m^{-1}·K^{-1}) plays a critical role in the LSSE measurement.[38,39] As a temperature gradient is applied across the ITO/YIG/GGG heterostructure, the huge thickness difference (ITO: 100 nm, YIG/GGG: 0.5 mm) leads to that most heat is dropped across the YIG/GGG substrate. Hence, the temperature gradient across the ITO/YIG interface is negligible, producing no spin currents and ISHE signal in ITO.[5,40–43] On the contrary, the remarkable difference of thermal conductivity between Pt (77.8 W·m^{-1}·K^{-1}) and YIG/GGG (6–9 W·m^{-1}·K^{-1}) causes a large temperature gradient across the Pt/YIG interface, giving rise to the generation of spin currents and the corresponding ISHE signal in Pt.[36,37] A weak $V_{\rm ISHE}$ signal has been observed in IrO_2/YIG, and attributed to the smaller $g_{\uparrow\downarrow}$ (1.2×10^{16} m^{-2}).[25] Usually, the smaller $g_{\uparrow\downarrow}$ originates from the rough interface of the layered heterostructures. However, the rough interface also gives rise to a large interfacial thermal resistance,[5,40–43] forming a sizable temperature gradient at the IrO_2/YIG interface and facilitating to introduce spin currents. Therefore, it is necessary to find a compromise between the interface mixing conductance $g_{\uparrow\downarrow}$ and interfacial thermal resistance via adjusting the interfacial structure so as to achieve large LSSE. It is expected to realize high spin to charge conversion for all oxide systems through interface structural modification in the future. Recently, Flebus and Cornelissen *et al.* suggested that a spin superfluidity can be generated in the bulk of YIG and manifest as SSE,[44–47] implying that there may be other factor hindering the visibility of the LSSE signal in our experiment. One possibility is that the spin mixing conductance may have a large negative temperature coefficient,[48,49] so that at higher measurement temperature, the magnon current is blocked by the interface, then the spin mixing conductance will be eliminated. Thereafter, we measured the thermal voltage of ITO/YIG as a function of H in the temperature range of 150 K to 300 K, but no visible ISHE signal was found. The LSSE measurement in the lower temperature regime will be performed in the future, so as to reveal the relative contribution of interface and YIG bulk toward ISHE.

4. Conclusion and perspectives

In summary, we investigated the ISHE in ITO/YIG by the methods of spin pumping and spin Seebeck effect. It is shown that the ISHE voltage can be generated in ITO by spin pumping under different magnetization configurations. Moreover, the enhancement of spin Hall angle and interfacial spin mixing conductance can be realized by appropriate thermal treatment. However, the ISHE voltage is hardly seen in the presence of a longitudinal temperature gradient, which can be ascribed to the almost equal thermal conductivity of ITO and YIG, as well as the specific interface structure, or the large negative temperature dependent spin mixing conductance. These results provide vital information to realize effective spin-current-driven devices by engineering the interfacial structures.

References

[1] Uchida K, Takahashi S, Harii K, Ieda J, Koshibae W, Ando K, Maekawa S and Saitoh E 2008 *Nature* **455** 778

[2] Uchida K, Xiao J, Adachi H, Ohe J, Takahashi S, Ieda J, Ota T, Kajiwara Y, Umezawa H, Kawai H, Bauer G E W, Maekawa S and Saitoh E 2010 *Nat. Mater.* **9** 894

[3] Jaworski C M, Yang J, Mack S, Awschalom D D, Myers R C and Heremans J P 2011 *Phys. Rev. Lett.* **106** 186601

[4] Qu D, Huang S Y, Hu J, Wu R and Chien C L 2013 *Phys. Rev. Lett.* **110** 067206

[5] Schreier M, Kamra A, Weiler M, Xiao J, Bauer G E W, Gross R and Goennenwein S T B 2013 *Phys. Rev. B* **88** 094410

[6] Tserkovnyak Y, Brataas A and Bauer E W 2002 *Phys. Rev. Lett.* **88** 117601

[7] Saitoh E, Ueda M, Miyajima H and Tatara G 2006 *Appl. Phys. Lett.* **88** 182509

[8] Ando K, Kajiwara Y, Takahashi S, Maekawa S, Takemoto K, Takatsu M and Saitoh E 2008 *Phys. Rev. B* **78** 014413

[9] Mosendz O, Pearson J E, Fradin F Y, Bauer G E W, Bader S D and Hoffmann A 2010 *Phys. Rev. Lett.* **104** 046601

[10] Nakayama H, Ando K, Harii K, Yoshino T, Takahashi R, Kajiwara Y, Uchida K, Fujikawa Y and Saitoh E 2012 *Phys. Rev. B* **85** 144408

[11] Du C, Wang H, Chris Hammel P and Yang F 2015 *J. Appl. Phys.* **117** 172603

[12] Dyakonov M I and Perel V I 1971 *Phys. Lett. A* **35** 459

[13] Hirsch J E 1999 *Phys. Rev. Lett.* **83** 1834

[14] Zhang S 2000 *Phys. Rev. Lett.* **85** 393

[15] Schliemann J and Loss D 2004 *Phys. Rev. B* **69** 165315

[16] Sinova J, Culcer D, Niu Q, Sinitsyn N A, Jungwirth T and MacDonald A H 2004 *Phys. Rev. Lett.* **92** 126603

[17] Rashba E I 2004 *Phys. Rev. B* **70** 161201(R)

[18] Mishchenko E G, Shytov A V and Halperin B I 2004 *Phys. Rev. Lett.* **93** 226602

[19] Wunderlich J, Kastner B, Sinova J and Jungwirth T 2005 *Phys. Rev. Lett.* **94** 047204

[20] Tserkovnyak Y, Brataas A, Bauer G E W and Halperin B I 2005 *Rev. Mod. Phys.* **77** 1375

[21] Shi J, Zhang P, Xiao D and Niu Q 2006 *Phys. Rev. Lett.* **96** 076604

[22] Fujiwara K, Fukuma Y, Matsuno J, Idzuchi H, Niimi Y, Otani Y and Takagi H 2013 *Nat. Commun.* **4** 2893

[23] Qiu Z, Kajiwara Y, Ando K, Fujikawa Y, Uchida K, Tashiro T, Harii K, Yoshino T and Saitoh E 2012 *Appl. Phys. Lett.* **100** 022402

[24] Qiu Z, An T, Uchida K, Hou D, Shiomi Y, Fujikawa Y and Saitoh E 2013 *Appl. Phys. Lett.* **103** 182404

[25] Qiu Z, Hou D, Kikkawa T, Uchida K and Saitoh E 2015 *Appl. Phys. Express* **8** 083001

[26] Yin S L, Mao Q, Meng Q Y, Li D and Zhao H W 2013 *Phys. Rev. B* **88** 064410

[27] Kalarickal S S, Krivosik P, Wu M Z, Patton C E, Schneider M L, Kabos P, Silva T J and Nibarger J P 2006 *J. Appl. Phys.* **99** 093909

[28] Azevedo A, Vilela-Leão L H, Rodríguez-Suárez R L, Lacerda Santos A F and Rezende S M 2011 *Phys. Rev. B* **83** 144402

[29] Shikoh E, Ando K, Kubo K, Saitoh E, Shinjo T and Shiraishi M 2013 *Phys. Rev. Lett.* **110** 127201

[30] Rojas-Sanchez J C , Cubukcu M, Jain A, Vergnaud C, Portemont C, Ducruet C, Barski A, Marty A, Vila L, Attane J P , Augendre E, Desfonds G, Gambarelli S, Jaffres H, George J M and Jamet M 2013 *Phys. Rev. B* **88** 064403

[31] Weiler M, Althammer M, Schreier M, Lotze J, Pernpeintner M, Meyer S, Huebl H, Gross R, Kamra A, Xiao J, Chen Y T , Jiao H, Bauer G E W and Goennenwein S T B 2013 *Phys. Rev. Lett.* **111** 176601

[32] Layadi A 2002 *Phys. Rev. B* **65** 104422

[33] Inoue H Y, Harii K, Ando K, Sasage K and Saitoh E 2007 *J. Appl. Phys.* **102** 083915

[34] Uchida K I, Adachi H, Ota T, Nakayama H, Maekawa S and Saitoh E 2010 *Appl. Phys. Lett.* **97** 172505

[35] Kikkawa T, Uchida K, Shiomi Y, Qiu Z, Hou D, Tian D, Nakayama H, Jin X F and Saitoh E 2013 *Phys. Rev. Lett.* **110** 067207

[36] Uchida K, Ishida M, Kikkawa T, Kirihara A, Murakami T and Saitoh E 2014 *J. Phys.: Condens. Matter* **26** 343202

[37] Sola A, Kuepferling M, Basso V, Pasquale M, Kikkawa T, Uchida K and Saitoh E 2015 *J. Appl. Phys.* **117** 17C510

[38] Ashida T, Miyamura A, Oka N, Sato Y, Yagi T, Taketoshi N, Baba T and Shigesato Y 2009 *J. Appl. Phys.* **105** 073709

[39] Slack G A and Oliver D W 1971 *Phys. Rev. B* **4** 592

[40] Swartz E T and Pohl R O 1987 *Appl. Phys. Lett.* **51** 2200

[41] Chen J, Zhang G and Li B 2012 *J. Appl. Phys.* **112** 064319

[42] Qiu Z, Hou D, Uchida K and Saitoh E 2015 *J. Phys. D. Appl. Phys.* **48** 164013

[43] Burrowes C, Heinrich B, Kardasz B, Montoya E A, Girt E, Sun Y, Song Y Y and Wu M Z 2012 *Appl. Phys. Lett.* **100** 092403

[44] Giles B L, Yang Z, Jamison J S, Gomez-Perez J M, Vélez S, Hueso L E, Casanova F and Myers R C 2017 *Phys. Rev. B* **96** 180412(R)

[45] Flebus B, Bender S A, Tserkovnyak Y and Duine R A 2016 *Phys. Rev. Lett.* **116** 117201

[46] Cornelissen L J, Peters K J H, Bauer G E W, Duine R A and Wees B J 2016 *Phys. Rev. B* **94** 014412

[47] Iguchi R, Uchida K-ichi, Daimon S and Saitoh E 2017 *Phys. Rev. B* **95** 174401

[48] Wang S, Zou L, Zhang X, Cai J, Wang S, Shen B and Sun J 2015 *Nanoscale* **7** 17812

[49] Atsarkin V A, Borisenko I V, Demidov V V and Shaikhulov T A 2018 *J. Phys. D: Appl. Phys.* **51** 245002